International Journal of Bridge Engineering (IJBE), Vol. 3, No. 1, (2015), pp. 11-32

A MATHEMATICAL MODEL FOR CABLES PROVIDED WITH DAMPERS

Ioannis G. Raftoyiannis, George T. Michaltsos

National Technical University of Athens, Dept. of Civil Engineering, Greece
e-mail: rafto@central.ntua.gr

ABSTRACT: Cables are efficient structural elements that are used in cable-stayed bridges, suspension bridges and other cable structures. These cables are subjected to environmental excitations such as rain - wind induced vibrations. Rain-wind induced vibrations of stay-cables may occur at different cable eigenfrequencies. Therefore, external transverse dampers have to be designed for several target cable modes in order to drastically decrease the oscillations amplitude. For the analytical study of such problems are, usually, used finite series or sinus forms. In this paper the real eigenfrequencies and shape functions are determined and used. This paper aims to study the optimum position and characteristics of such a damper, and its influence on the cable's vibrations, using the real cable modes and taking into account the cable's flexural rigidity.

KEY WORDS: Cables; rain-wind; induced vibrations; dampers

1 INTRODUCTION

Cable stayed bridges have been known since the beginning of the 18th century, but they have been of great interest only in the last fifty years, particularly due to their special shape and also because they are an alternative solution to suspension bridges for long spans. The main reasons for this delay were the difficulties in their static and dynamic analysis, the various non-linearities, and the absence of computational capabilities, the lack of high strength materials and the lack of construction techniques. There is a great number of studies, concerning the static behavior [1-8], the dynamic analysis [9-17], or the stability of cable-stayed bridges [18-21].

A significant problem, which arose from the praxis, is the cables' rain-wind induced vibrations. Large amplitude Rain-Wind-Induced-Vibrations (RWIV) of stay cables are a challenging problem in the design of cable-stayed bridges. Such phenomena were first observed on the Meikonishi bridge in Nagoya, Japan [22] and also later on other such bridges, as for instance on the fully steel Erasmus bridge in Rotterdam, the Netherlands (1996) and the Second Severn Crossing, connecting England and Wales [23]. It was found that the cables, which were stable under wind action only, were oscillating under a combined influence of rain and wind, leading to large amplitude motions, even for lightto-moderate simultaneous rain and wind action. The frequency of the observed vibrations was much lower than the critical one of the vortex-induced vibrations, while it was also perceived that the cable oscillations took place in the vertical plane mostly in single mode; for increasing cable length however, higher modes (up to the 4th) appeared. Most importantly, during the oscillations a water rivulet appeared on the lower surface of the cable, which was characterized by a leeward shift and vibrated in circumferential directions [22, 24, 25].

The so-produced vibrations can cause reduced life of the cable and connection due to fatigue or rapid progress of the corrosion.

Several methods, including aerodynamic or structural means, have been investigated in order to control the vibrations of bridge's stay cables. Aerodynamic methods, just as change of the cables' roughness were effective only for certain classes of vibration. Another method is the coupling of the stays with secondary wires, in order to reduce their effective length and thereby to avoid resonance. This method changes the bridge's aesthetics.

Another widely applied method is this of external dampers attached transverse to the stay-cables. Many researchers have proposed passive control of cables using viscous dampers.

The last method consist in a system of movable anchorage by using a Friction Pendulum Bearing or an Elastomeric bearing to replace the conventional fixed support of stay cables.

For the analytical study of such problems are, usually, used finite series or sinus forms. In this paper the real eigenfrequencies and shape functions are determined and used. This paper aims to study the optimum situation and characteristics of such a damper, and its influence on the cable's vibrations, using the real cable modes and taking into account the cable's flexural rigidity.

2. BASIC ASSUMPTIONS

a. The studied cable has, under the dead and live loads, the catenary shape elastic line, with displacements w_o and tensile forces T_o (see fig.1).

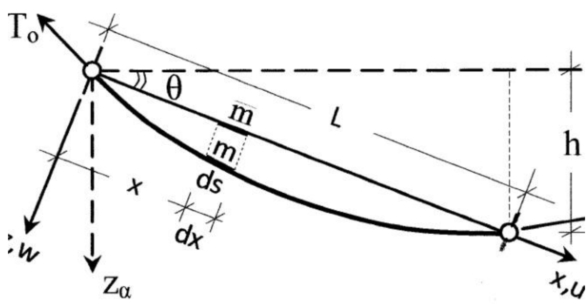

Figure 1: Cables and reference axes

b. Under the action of the dynamic loads $p_y(x,t)$ and $p_z(x,t)$, the cable takes the shape of figure 2, with additional displacements u_d, υ_d, w_d and tensile forces T_d.

c. The form of the cables (under static and dynamic loads) is a catenary curve, which because of its shallow form, can be replaced by a parabola of second-order.

d. The static and dynamic tensile forces are connected with the following relations:

$$\left.\begin{aligned} T(t) &= T_o + T_d(t) \\ H(t) &= H_o + H_d(t) \end{aligned}\right\} \qquad (1.1\ a,b)$$

where H, is the projection of T on x-axis.

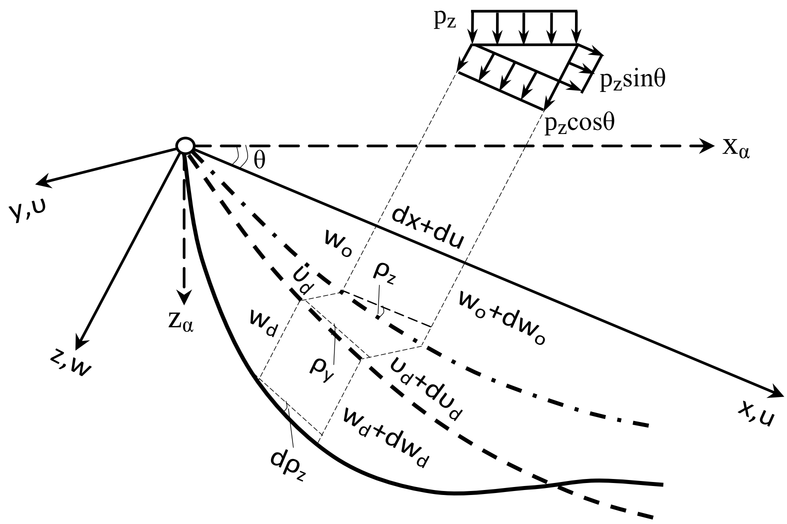

Figure 2: Deformation of the cable

e. The $\overline{m}(x)$ and m(s) of figure 1, are connected through the relation

$$\overline{m}(x) = m(s)\frac{ds}{dx} \qquad (1.2)$$

f. The studied cables are referred to the inclined axis system 0-xyz of fig.1.

3. THE EQUATIONS OF MOTION

3.1 Projection on xoz-plane

For a shallow form of the cable, the following relations are valid (see also fig. 2):

$$\left.\begin{aligned}&\cos\rho_z = dx/ds \cong 1\\&\sin\rho_z = dw/ds\\&\sin d\rho_z \cong 0\end{aligned}\right\} \qquad (2.1\ a,b)$$

3.1.1 Equilibrium of horizontal forces

Projecting on the xoz-plane and taking the equilibrium of horizontal forces we obtain:

$$-T\frac{dx}{ds}+T\frac{dx}{ds}+\partial\left(T\frac{dx}{ds}\right)+Q_z\frac{dw}{ds}-Q_z\frac{dw}{ds}-\partial\left(Q_z\frac{dw}{ds}\right)+p_x ds-c\dot{u}ds-m\ddot{u}ds=0,$$

or finally:

$$\frac{\partial H}{\partial s}-\frac{\partial}{\partial s}\left(Q_z\frac{dw}{ds}\right)-c\dot{u}-m\ddot{u}=-p_x(x,t) \qquad (2.2)$$

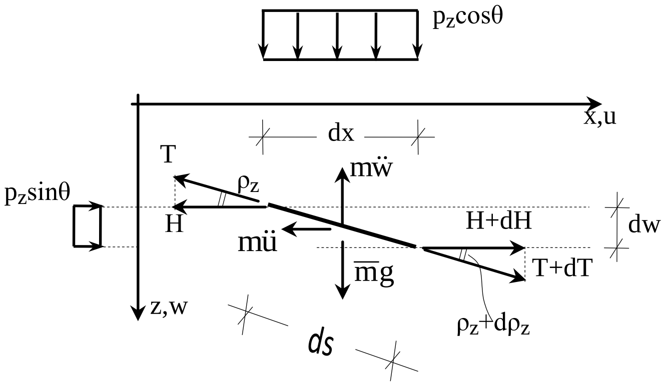

Figure 3: Projection on xoz-plane

3.1.2 Equilibrium of vertical forces

Projecting the on xoz-plane and taking the equilibrium of vertical forces we obtain:

$$-T\frac{\partial w}{\partial s}+T\frac{\partial w}{\partial s}+\partial\left(T\frac{\partial w}{\partial s}\right)-Q_z\frac{dx}{ds}+Q_z\frac{dx}{ds}+\partial\left(Q_z\frac{dx}{ds}\right)+\overline{m}gds+p_z ds-c\dot{w}ds-m\ddot{w}ds=0$$

or $$\frac{\partial}{\partial s}\left(T\frac{\partial w}{\partial s}\right)+\frac{\partial}{\partial s}\left(Q_z\frac{dx}{ds}\right)-c\dot{w}ds-m\ddot{w}ds=-\overline{m}gds-p_z ds \qquad (2.3a)$$

The equation of the static equilibrium is valid. That is: $\frac{\partial}{\partial s}\left(T_o \frac{\partial w_o}{\partial s}\right) = -\overline{m}g$, and equation (2.3a), taking into account that $\frac{\partial}{\partial t} w_o(x) = 0$, gives:

$$\frac{\partial}{\partial s}\left[T_o \frac{\partial w_d}{\partial s} + T_d \frac{\partial}{\partial s}(w_o + w_d)\right] + \frac{\partial Q_z}{\partial s} - c\dot{w}_d - m\ddot{w}_d = -p_z(x,t)$$

, which finally becomes to:

$$T_o \frac{\partial^2 w_d}{\partial x^2} + T_d\left(\frac{\partial^2 w_o}{\partial x^2} + \frac{\partial^2 w_d}{\partial x^2}\right) + \frac{\partial Q_z}{\partial s} - c\dot{w}_d - m\ddot{w}_d = -p_z(x,t) \tag{2.3b}$$

3.1.3 Equilibrium of moments

Equilibrium of moments gives:

$$\frac{\partial M_y}{\partial x} - Q_z = 0 \tag{2.4}$$

Because of (2.4), and remembering that $M_y = -EI_y \frac{\partial^2 w_d}{\partial x^2}$, equation (2.3b) becomes to:

$$EI_y \frac{\partial^4 w_d}{\partial x^4} - T_o \frac{\partial^2 w_d}{\partial x^2} - T_d\left(\frac{\partial^2 w_o}{\partial x^2} + \frac{\partial^2 w_d}{\partial x^2}\right) + c\frac{\partial w_d}{\partial t} + m\frac{\partial^2 w_d}{\partial t^2} = +p_z(x,t) \tag{2.5}$$

3.2 Projection on xoy-plane

3.2.1 Equilibrium of vertical forces

Projecting the on xoy-plane, taking the equilibrium of vertical forces and through a similar process like the one of §3.1.2 we obtain:

$$T_o \frac{\partial^2 \upsilon_d}{\partial x^2} + T_d \frac{\partial^2 \upsilon_d}{\partial x^2} + \frac{\partial Q_y}{\partial x} - c\dot{\upsilon}_d - m\ddot{\upsilon}_d = -p_y(x,t) \tag{2.6}$$

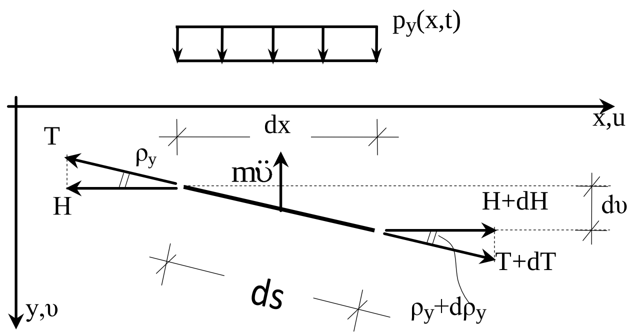

Figure 4: Projection on xoz-plane

3.2.2 Equilibrium of moments

Equilibrium of moments gives:

$$\frac{\partial M_z}{\partial x} - Q_y = 0$$

(2.7)

Because of (2.7), and remembering that $M_z = -E I_z \frac{\partial^2 \upsilon_d}{\partial x^2}$, equation (2.6) becomes to:

$$E I_z \frac{\partial^4 \upsilon_d}{\partial x^4} + T_o \frac{\partial^2 \upsilon_d}{\partial x^2} + T_d \frac{\partial^2 \upsilon_d}{\partial x^2} - c \frac{\partial \upsilon}{\partial t} - m \frac{\partial^2 \upsilon}{\partial t^2} = -p_y(x,t)$$

(2.8)

4. THE CABLES' DEFORMATION

The following relations are valid:

$$\left.\begin{aligned} & ds^2 = dx^2 + dw_o^2 , \\ & (ds + \Delta ds)^2 = (dx + \Delta dx)^2 + (\Delta d\upsilon)^2 + (dw_o + \Delta dw_o)^2 \end{aligned}\right\}$$

(3.1)

From the second of (3.1), neglecting the higher order terms we get: $\Delta dx = \Delta ds \cdot \frac{ds}{dx} - \Delta dw_o \frac{dw_o}{dx}$, and having that $\Delta dw_o = dw_d$, we obtain:

$$\Delta dx = \frac{\Delta ds}{ds} \cdot \frac{ds}{dx} \cdot \frac{ds}{dx} \cdot dx - \frac{dw_d}{dx} \cdot \frac{dw_o}{dx} \cdot dx$$

(3.2)

On the other hand we have: $\sigma = E \cdot \varepsilon$ or

$$\varepsilon = \frac{\sigma}{E} = \frac{T_d}{EA}$$

(3.3)

Because of (3.3), equation (3.2) becomes: $\Delta dx = \frac{T_d}{EA} \cdot \left(\frac{ds}{dx}\right)^2 \cdot dx - \frac{dw_d}{dx} \cdot \frac{dw_o}{dx} \cdot dx$

and using the condition: $\int_0^L \Delta dx = 0$, the above relation gives:

$$\frac{T_d}{EA} \int_0^L \frac{dx}{\cos^3 \rho_z} - \int_0^L \frac{dw_d}{dx} \cdot \frac{dw_o}{dx} \cdot dx = 0$$

or finally, after integration by members we obtain:

$$\left.\begin{aligned} T_d &= -\frac{w_o''}{L_o}\int_0^L w_d dx\,, \\ \text{with: } \quad L_o &= \int_0^L \frac{dx}{EA\cos^3\rho_z} \end{aligned}\right\} \tag{3.4a,b}$$

5. CATENARY AND THE PARABOLA APPROACH

It is necessary to determine the form w_o of a cable in rest. In this case we have: $p_z(x,t) = p_y(x,t) = 0$, $u = \upsilon = 0$, $w = w_o(x)$ and $\frac{dQ_z}{ds} \cong 0$, because $T >> Q_z$.

Therefore, equation (2.2) gives: $\frac{\partial H_o}{\partial s} = 0$, that means

$H_o = \text{Constant}$

(4.1)

On the other hand, equation (2.3a) gives: $\frac{\partial}{\partial s}\left(T_o\frac{\partial w_o}{\partial s}\right) = -\overline{m}g$ or

$\frac{\partial}{\partial s}\left(T_o \cdot \frac{dx}{ds}\cdot\frac{dw_o}{dx}\right) = \frac{\partial}{\partial s}\left(H_o \cdot \frac{dw_o}{dx}\right) = -\overline{m}\cdot g$, or finally:

$H_o \cdot \frac{d^2 w_o}{dx^2} = -\overline{m}\cdot g = -m\cdot g\cdot\frac{ds}{dx}$

(4.2)

It is usual to use the parabola as a curve that is very close to the catenary one, especially for shallow forms of cables. For a cable's shallow form (i.e. $ds \approx dx$), the equation of a parabola passing from the points (0,0), (L,0) and having $w_o'' = -\frac{\overline{m}g}{H_o}$ (from eq.4.2), is given by the following formula:

$$w_o(x) = \frac{\overline{m}g}{2H_o}\cdot x\cdot(L-x) \tag{5.1}$$

A comparison between the parabolic form of a cable (as the used in C-S-Bridges) and the catenary one, shows that the differences of the two carves' sags amount up to 0.02%.

6. EIGENFREQUENCIES AND SHAPE FUNCTIONS

For the analytical study of the dynamic behavior of cables usually are used finite series of sinus form.

In order to determine a range of functions that will satisfy the boundary conditions and will approach, as possible best, the real form of a vibrating

cable, we will study the freely vibrating cable, neglecting the influence of their rigidity.
Considering the freely vibrating cable, which of course is unloaded from external loads, the dynamic deformations w_d and υ_d will be significantly smaller than the static ones.
Therefore, the equations of motion can be written as follows:

$$\left.\begin{aligned} & T_o w_d'' + T_d w_o'' = c\dot{w}_d + m\ddot{w}_d \\ & T_o \upsilon_d'' = c\dot{\upsilon}_d + m\ddot{\upsilon}_d \\ & T_d = -\frac{w_o''}{L_o}\int_0^L w_d dx\,, \quad \text{with :} \quad L_o = \int_0^L \frac{dx}{EA\cos^3\rho_z} \end{aligned}\right\} \qquad (6.1a,b,c,d)$$

6.1 The vertical motion

Equation (6.1a), because of (6.1c) is written:

$$T_o w_d'' - c\dot{w}_d - m\ddot{w}_d - \frac{w_o''^2}{L_o}\cdot\int_0^L w_d dx = 0 \qquad (6.2)$$

We are searching for a solution of separate variables under the form:

$$w_d(x,t) = W(x)\cdot\Phi(t) \qquad (6.3)$$

Therefore, equation (6.2) becomes:

$$\frac{T_o W'' - \dfrac{w_o''^2}{L_o}\cdot\displaystyle\int_0^L W dx}{mW} = \frac{\ddot{\Phi} + \dfrac{c}{m}\dot{\Phi}}{\Phi} = -\omega_w^2 \qquad (6.4)$$

From (6.4), we get the following uncoupled equations:

$$\left.\begin{aligned} & W'' + \frac{m\omega_w^2}{T_o}W = \frac{w_o''^2}{T_o L_o}\int_0^L W dx \\ & \ddot{\Phi} + \frac{c}{m}\dot{\Phi} + \omega_w^2\Phi = 0 \end{aligned}\right\} \qquad (6.5a,b)$$

Equation (6.5a), has the solution:

$$\left.\begin{aligned} & W(x) = c_1\sin\lambda_w x + c_2\cos\lambda_w x + \frac{w_o''^2}{\lambda_w^2 T_o L_o}\cdot\int_0^L W(x)dx \\ & \text{with :} \quad \lambda_w^2 = \frac{m\omega_w^2}{T_o} \end{aligned}\right\} \qquad (6.6a,b)$$

Equation (6.6a) is an integral-differential one with degenerate kernel, i.e. the classic equation of Hammerstein.
Integrating the above equation, we finally obtain:

$$\int_0^L W dx = \frac{\lambda_w T_o L_o}{\lambda_w^2 T_o L_o - w_o''^2 L} \cdot [c_1 \sin(1-\cos\lambda_w L) + c_2 \sin\lambda_w L]$$

Therefore, equation (6.6a) becomes:

$$\left.\begin{aligned} & W(x) = c_1[\sin\lambda_w x + G(1-\cos\lambda_w L)] + c_2[\cos\lambda_w x + G\sin\lambda_w L] \\ & \text{where:} \quad G = \frac{w_o''^2}{\lambda_w(\lambda_w^2 T_o L_o - w_o''^2 L)} \end{aligned}\right\} \tag{6.7a,b}$$

The boundary conditions are:

$$W(0) = W(L) = 0 \tag{6.8a,b}$$

Introducing equation (6.7a) into the above (6.8) we get the following system:

$$\left.\begin{aligned} & G(1-\cos\lambda_w L)\cdot c_1 + (1+G\sin\lambda_w L)\cdot c_2 = 0 \\ & [\sin\lambda_w L + G(1-\cos\lambda_w L)]\cdot c_1 + [\cos\lambda_w L + G\sin\lambda_w L]\cdot c_2 = 0 \end{aligned}\right\} \tag{6.9a,b}$$

In order for the above system to have a non-trivial solution, the determinant of the coefficients of the unknowns must be zero. This condition concludes to the following eigenfrequencies equation:

$$2G\cos\lambda_w L - \sin\lambda_w L - 2G = 0 \tag{6.10}$$

Finally from (6.9) and (6.10) one can determine the following form of shape functions:

$$W_n(x) = c_1 \cdot \left[\sin\lambda_{wn} x - \frac{G_n(1-\cos\lambda_{wn} L)}{1+G_n \sin\lambda_{wn} L}\cdot\cos\lambda_{wn} x + \frac{G_n(1-\cos\lambda_{wn} L)}{1+G_n \sin\lambda_{wn} L}\right] \tag{6.11}$$

Easily one can prove that the following orthogonality condition is valid:

$$\int_0^L W_n W_k dx = \begin{cases} 0 & \text{for} \quad n \neq k \\ \Gamma_n & \text{"} \quad n = k \end{cases} \tag{6.12}$$

6.2 The lateral motion

Equation (6.1b), is written:

$$T_o \upsilon_d'' - c\dot{\upsilon}_d - m\ddot{\upsilon}_d = 0 \tag{6.13}$$

Following the previous procedure and searching for a solution of the form $\upsilon_d(x,t) = V(x)R(t)$, we conclude to the following equations:

$$\left.\begin{aligned} & T_o V'' + m\omega_\upsilon^2 V = 0 \\ & \ddot{R} + \frac{c}{m}\dot{R} + \omega_\upsilon^2 R = 0 \end{aligned}\right\} \tag{6.14a,b}$$

Equation (6.14a), has the solution:

$$\left.\begin{aligned} & V(x) = d_1 \sin\lambda_\upsilon x + d_2 \cos\lambda_\upsilon x \\ & \text{with:} \quad \lambda_\upsilon^2 = \frac{m\omega_\upsilon^2}{T_o} \end{aligned}\right\} \tag{6.15a,b}$$

The boundary conditions are $V(0)=V(L)=0$, which finally give:

$$\left.\begin{array}{l} V_n(x)=d_1\sin\dfrac{n\pi x}{L}\,,\quad \omega_{\upsilon n}^2=\dfrac{n^2\pi^2 T_o}{mL^2} \end{array}\right\} \qquad (6.16a,b)$$

7. THE FORCED VIBRATING CABLE

According the acceptances of §1, the equations of motion of a cable subjected to external dynamic loadings and supported by dampers at a point of its length can be written as follows.

$$\left.\begin{array}{l} EI_y w_d'''' - T_o w_d'' - T_d w_o'' + c\dot{w}_d + m\ddot{w}_d = p_z(x)f(t) - c_d\dot{w}_d\delta(x-\alpha_d) \\ EI_z \upsilon_d'''' + T_o\upsilon_d'' - c\dot{\upsilon}_d - m\ddot{\upsilon}_d = -p_y(x)f(t) + c_d\dot{\upsilon}_d\delta(x-\alpha_d) \\ T_d = -\dfrac{w_o''}{L_o}\cdot\displaystyle\int_0^L w_d\,dx \end{array}\right\} \qquad (7.1a,b,c)$$

where c_d is the damper's coefficient, α_d the damper's position and $\delta(x)$ the Dirac's delta function (see figure 5)

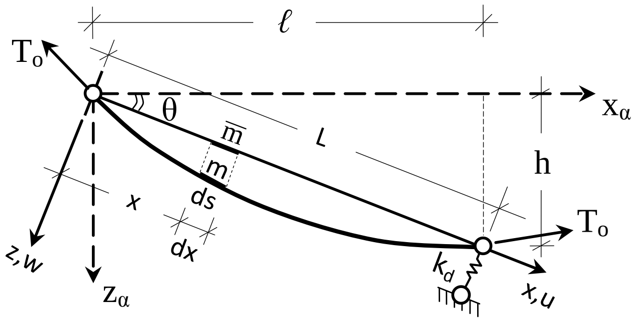

Figure 5: Cable and damper

7.1. The vertical motion

In order to solve equation (7.1a), we are searching for a solution of the form:

$$w_d(x,t)=\sum_n W_n(x)\cdot\Phi_n(t) \qquad (7.2)$$

where $W_n(x)$ are the shape functions given by equation (6.11) and $\Phi_n(t)$ are unknown time functions under determination. Introducing (7.2) into (7.1a) we get:

$$\left.\begin{aligned}&EI_y\sum_n W_n''''\Phi_n - H_o\sum_n W_n''\Phi_n + \frac{w_o''^2}{L_o}\cdot\int_0^L\sum_n W_n\Phi_n dx + c\sum_n W_n\dot{\Phi}_n + m\sum_n W_n\ddot{\Phi}_n = \\ &\qquad = p_z(x)f(t) - c_d\sum_n W_n\dot{\Phi}_n\delta(x-\alpha_d)\end{aligned}\right\} \tag{7.3a}$$

Remembering that W_n satisfies equation (6.5a), the above becomes:

$$\left.\begin{aligned}&EI_y\sum_n W_n''''\Phi_n + m\sum_n \omega_{wn}^2 W_n\Phi_n + c\sum_n W_n\dot{\Phi}_n + m\sum_n W_n\ddot{\Phi}_n = \\ &\qquad = p_z(x)f(t) - c_d\sum_n W_n\dot{\Phi}_n\delta(x-\alpha_d)\end{aligned}\right\} \tag{7.3b}$$

Multiplying (7.3b) by W_k, integrating the resulting from 0 to L and taking into account the orthogonality condition we obtain:

$$\left.\begin{aligned}&EI_y\Phi_k\int_0^L W_k''^2 dx + m\omega_{wn}^2\Phi_k\int_0^L W_k^2 dx + c\dot{\Phi}_k\int_0^L W_k^2 dx + m\ddot{\Phi}_k\int_0^L W_k^2 dx = \\ &\qquad = f(t)\int_0^L p_z W_k dx - c_d W_k(\alpha_d)\sum_n W_n(\alpha_d)\dot{\Phi}_n\end{aligned}\right\}$$

which finally becomes:

$$\left.\begin{aligned}&\ddot{\Phi}_k + \frac{c}{m}\dot{\Phi}_k + \frac{EI_y\int_0^L W_k''^2 dx + m\omega_{wn}^2\int_0^L W_k^2 dx}{m\int_0^L W_k^2 dx}\Phi_k + \frac{c_d W_k(\alpha_d)}{m\int_0^L W_k^2 dx}\sum_n W_n(\alpha_d)\dot{\Phi}_n = \\ &\qquad = \frac{\int_0^L p_z(x)W_k dx}{m\int_0^L W_k^2 dx}f(t)\end{aligned}\right\} \tag{7.4}$$

for k= 1 to n.

In order to solve the above differential system, we use the Lagrange transformation.

Thus, we set:

$$\left.\begin{aligned}&L\Phi_k(t) = \varphi(s)\\ &Lf(t) = F(s)\end{aligned}\right\} \tag{7.5a,b}$$

With initial conditions $\Phi_k(0) = \dot{\Phi}_k(0) = 0$, equation (7.4) becomes:

$$\left.\begin{aligned}
&A_{k1}\varphi_1 + A_{k2}\varphi_2 + \cdots\cdots + A_{kn}\varphi_n = B_k \\
&\text{where:}\quad A_{k\rho} = \frac{c_d W_k(\alpha_d)}{m\int_0^L W_k^2 dx}\cdot W_\rho(\alpha_d)\cdot s \\
&\qquad A_{kk} = s^2 + \left[\frac{c}{m} + \frac{c_d W_k^2(\alpha_d)}{m\int_0^L W_k^2 dx}\right]\cdot s + \frac{E\,I_y\int_0^L W_k''^2 dx + m\omega_{wn}^2\int_0^L W_k^2 dx}{m\int_0^L W_k^2 dx} \\
&\qquad B_k = \frac{\int_0^L p_z(x) W_k dx}{m\int_0^L W_k^2 dx}\cdot F(s) \\
&\text{with:}\quad k = 1 \quad \text{to} \quad n \\
&\qquad\quad \rho = 1 \quad \text{to} \quad n
\end{aligned}\right\}$$

(7.6a,b,c,d)

Solving the system (7.6a) we get $\varphi_k(s)$ and therefore:

$$\Phi_k(t) = L^{-1}\varphi_k(s) \tag{7.7}$$

7.2. The lateral motion

In order to solve equation (7.1b), we are searching for a solution of the form:

$$\upsilon_d(x,t) = \sum_n V_n(x)\cdot R_n(t) \tag{7.8}$$

with V_n from (6.16a).

Following a similar procedure like the one of §7.1, and putting:

$$\left.\begin{aligned} LR_k(t) &= r_k(s) \\ Lf(t) &= F(s) \end{aligned}\right\} \tag{7.9a,b}$$

We conclude to the following system:

$$\left.\begin{aligned}
&A_{k1}r_1 + A_{k2}r_2 + \cdots\cdots + A_{kn}r_n = B_k \\
&\text{where:}\quad A_{k\rho} = \frac{c_d V_k(\alpha_d)}{m\int_0^L V_k^2 dx}\cdot V_\rho(\alpha_d)\cdot s \\
&\qquad A_{kk} = s^2 + \left[\frac{c}{m} + \frac{c_d V_k^2(\alpha_d)}{m\int_0^L V_k^2 dx}\right]\cdot s + \frac{EI_y\int_0^L V_k''^2 dx + m\omega_{wn}^2\int_0^L V_k^2 dx}{m\int_0^L V_k^2 dx} \\
&\qquad B_k = \frac{\int_0^L p_y(x)V_k dx}{m\int_0^L V_k^2 dx}\cdot F(s) \\
&\text{with:}\quad k = 1 \quad \text{to} \quad n \\
&\qquad\ \ \rho = 1 \quad \text{to} \quad n
\end{aligned}\right\}$$

(7.10a,b,c,d)

Solving the system (7.10a), we get $r_k(s)$ and therefore:

$$R_k(t) = L^{-1}r_k(s) \tag{7.11}$$

8. NUMERICAL RESULTS AND DISCUSSION

8.1. The cables

We consider a c-s-bridge with dense distribution of cables.

We separate a cable with tension T_o=300000 dN/cable, and cross-section area F=7.5*10^{-3}m^2, diameter D=0.13 m, weight G=70 dN/m and mass per unit length m=7kg/m.

According to [2] one can determine the corresponding moment of inertia of the cable: $I = 0.8\cdot 10^{-5}\,m^4$. We will study cables with lengths L=150 m, 250 m, and 350 m.

8.2. The rain-wind combination

It has been observed that the rain-wind-induced vibration in bridge cables usually occurs in the frequency range from 0.5 to 4 sec^{-1}, [23, 25]. For the study of the vibration of a cable under the action of a rain-wind combination we choose the following loading:

$p = p(x)\cdot f(t) = 20\cdot \sin\omega t$. where ω= 1, 2, 3, 4 sec^{-1}.

8.3. Behavior of the cables without a damping system

Using equation (6.10), we determine the eigenfrequencies of the above considered cables, as they are shown in the following table 1.

TABLE 1

	m=7kg/m , T_o=300000 dN		
	L=150m	**L=250m**	**L=350m**
ω_1	4.4697	2.8186	2.1507
ω_2	8.6716	5.2029	3.7164
ω_3	13.0125	7.8130	5.5868
ω_4	17.3432	10.4059	7.4328
ω_5	21.6801	13.0093	9.2936

In figures 6 to 8 they are shown the oscillations of each one cable of L=150, L=250 and L=350m, subjected to loadings acting with frequencies ω=1, 2, 3, 4 sec^{-1}.

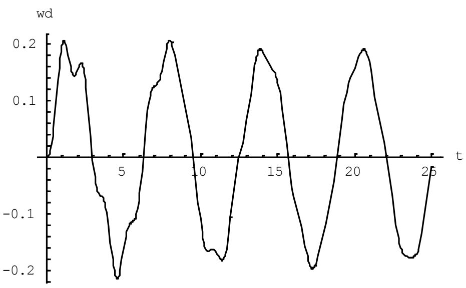

p=20·Sin(1·t)

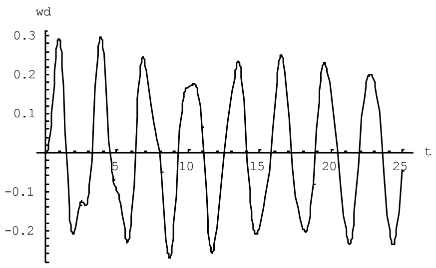

p=20·Sin(2·t)

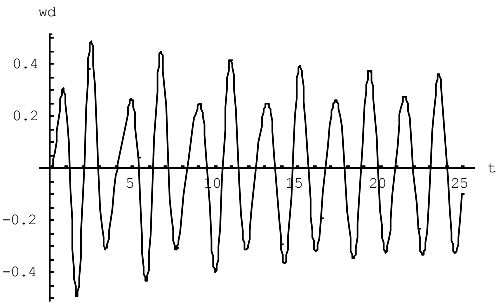

p=20·Sin(3·t)

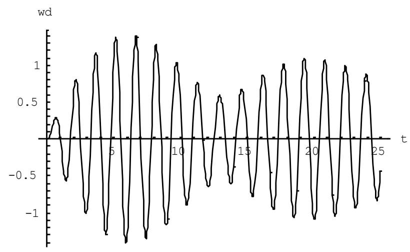

(*) p=20·Sin(4·t)

Figure 6: Oscillations of the cable of length L=150m, without any damping system. (*) In this case, we have big deformations, because the eigenfrequency of the external load is near to the first one of the cable (that is ω_1 =4.47 sec^{-1}).

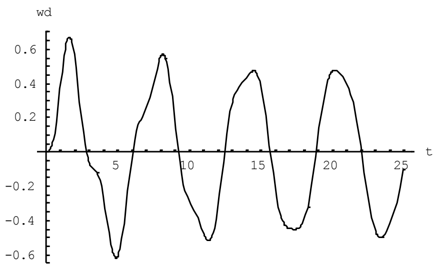

p=20·Sin(1·t)

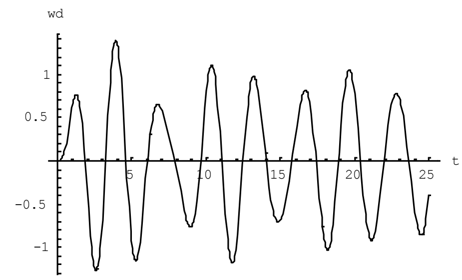

p=20·Sin(2·t)

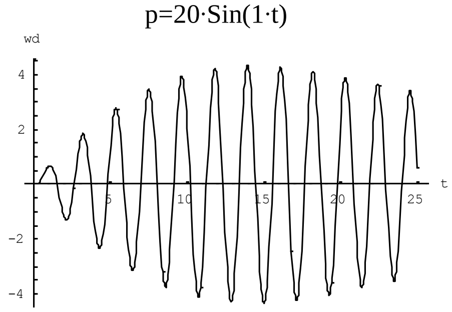

(*) p=20·Sin(3·t)

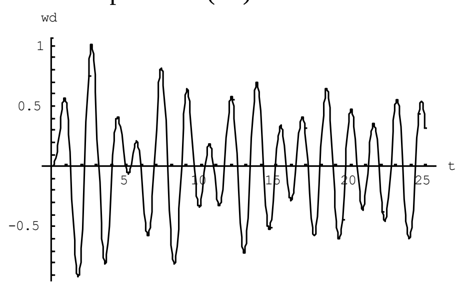

p=20·Sin(4·t)

Figure 7: Oscillations of the cable of length L=250m, without any damping system. (*) In this case, we have big deformations, because the eigenfrequency of the external load is near to the first one of the cable (that is ω_1 =2.82 sec^{-1}).

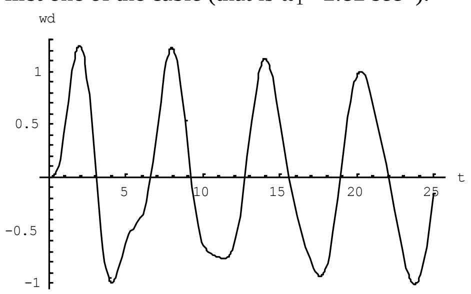

p=20·Sin(1·t)

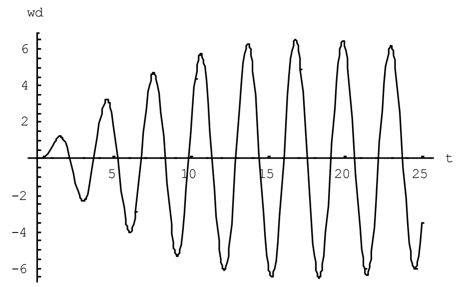

(*) p=20·Sin(2·t)

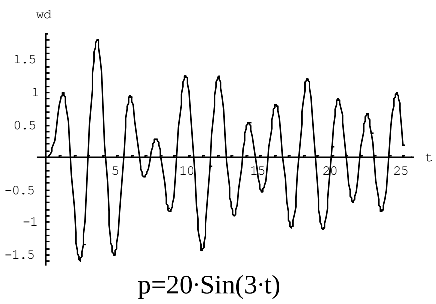

p=20·Sin(3·t)

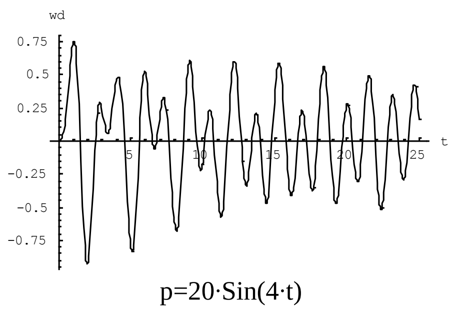

p=20·Sin(4·t)

Figure 8: Oscillations of the cable of length L=350m, without any damping system. (*) In this case, we have big deformations, because the eigenfrequency of the external load is near to the first one of the cable (that is ω_1 =2.15 sec^{-1}).

Finally, in figure 9, we see the influence of the cable's moment of inertia I on the deformations of a cable of L=150m. We note, that for the usual values of $I=0.4*10^{-5}$ to $1.5*10^{-5}$, this influence is negligible (~0.1%), while becomes notable for $I > 100*10^{-5}$.

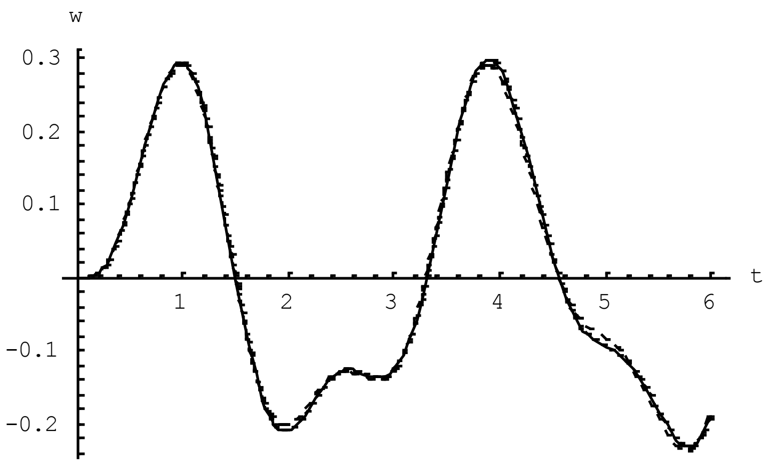

Figure 9: The influence of I. (___ I=0, ……. $I=1*10^{-5}$, - - - $I=50*10^{-5}$)

8.4. The dampers

Let us consider now the cable of figure 5, which is provided by a damper of constant c_d, attached at the point $x=a_T*L$.
We study three kind of dampers with constants c_d=0.01, 0,10, and 0.5 $dN \cdot \sec / mm$, which are placed at α_T=0.99 L, 0.98 L and 0.97 L.

It is obvious that for α_T=0.97 L and for cables of great length the damper will be placed in a distance relatively great from the cable's anchorage. This distance has, of course, a maximum that amounts on about 10 to 20m from the cable's anchorage.
Therefore, mainly for long cables, the solution of dampers for diminishing the cable's oscillations becomes ineffective.
The cables studied, have the characteristics of §8.1 and lengths 150, 250 and 350m.
Finally the used exciting external loading, for the studied examples, is given by the equation:
p=20*sin3t.
In the plots of figure 10, we see the oscillations of the middle of a cable of length L=150m for different dampers placed at different positions. We observe that the damping system becomes more effective as it is removed from the cable's anchorage.

Comparing these diagrams to the ones of figure 6, we see that the decreasing of the oscillations amounts from ~2% (α_T=0.99L) to ~10% (α_T=0.97L) and c_d=0.01, from ~10% (α_T=0.99L) to ~40% (α_T=0.97L) and c_d=0.1, and from ~30% (α_T=0.99L) to ~60% (α_T=0.97L) and c_d=0.5.

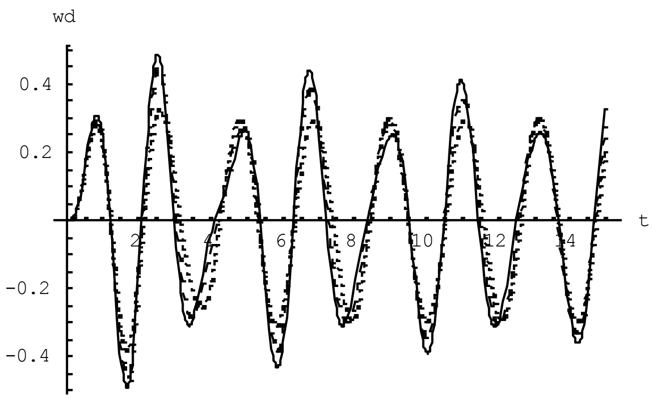

aT=0.99

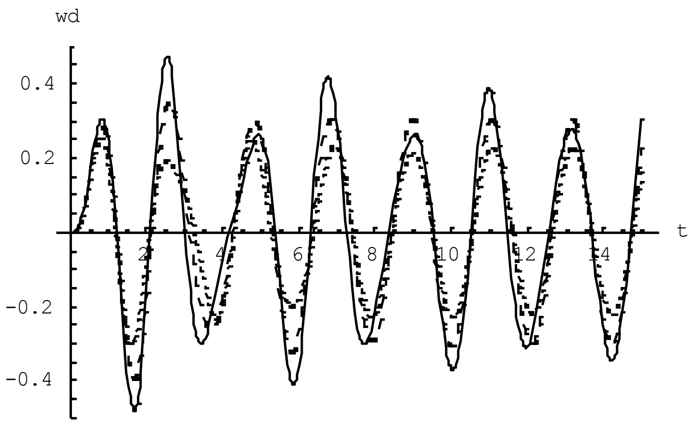

aT=0.98

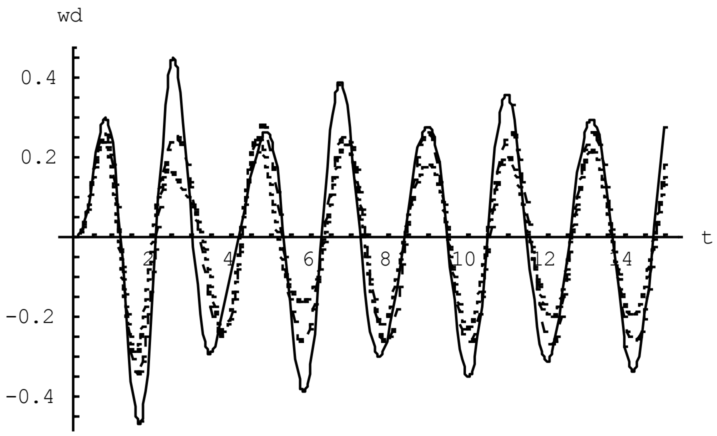

aT=0.97

Figure 10: Cables L=150m, with dampers (___ cd=0.01, _ _ cd=0.1, - - - cd=0.5 dN sec/mm)

In the plots of figure 11, we see the oscillations of the middle of a cable of length L=250m for different dampers placed at different positions. Comparing these diagrams to the ones of figure 7, we see that the decreasing of the oscillations amounts from ~0% (α_T=0.99L) to ~22% (α_T=0.97L) and c_d=0.01, from ~15% (α_T=0.99L) to ~45% (α_T=0.97L) and c_d=0.1, and from ~40% (α_T=0.99L) to ~30% (α_T=0.97L) and c_d=0.5.
We observe that as the damper becomes stronger its effective diminishes for α_T>0.98L.

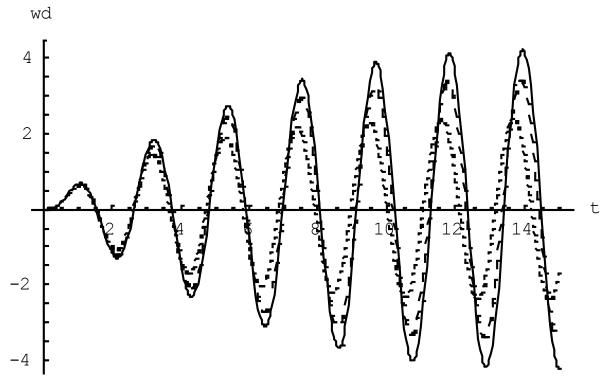

aT=0.99

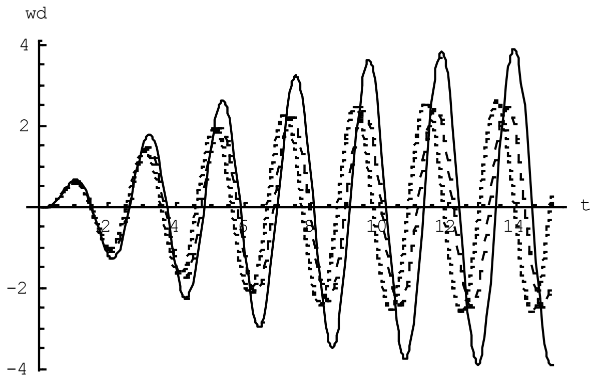

aT=0.98

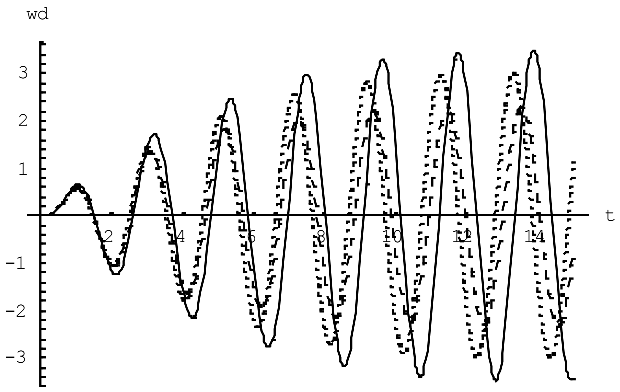

aT=0.97

Figure 11: Cables L=250m, with dampers (___ cd=0.01, _ _ cd=0.1, - - - cd=0.5 dN sec/mm)

Noting that the studied loading p=p*sin3t, produces very large oscillations because the ω=3 approaches the first eigenfrequency ω_1 =2.81 sec^{-1}

In the plots of figure 12, we see the oscillations of the middle of a cable of length L=350m for different dampers placed at different positions. Comparing these diagrams to the ones of figure 8, we see that the decreasing of the oscillations amounts from ~3% (α_T=0.99L) to ~7% (α_T=0.97L) and c_d=0.01, from ~8% (α_T=0.99L) to ~20% (α_T=0.97L) and c_d=0.1, and from ~10% (α_T=0.99L) to ~15% (α_T=0.97L) and c_d=0.5.

We observe that for some combinations c_d and α_T the softer dampers are more efficient than the stronger ones.

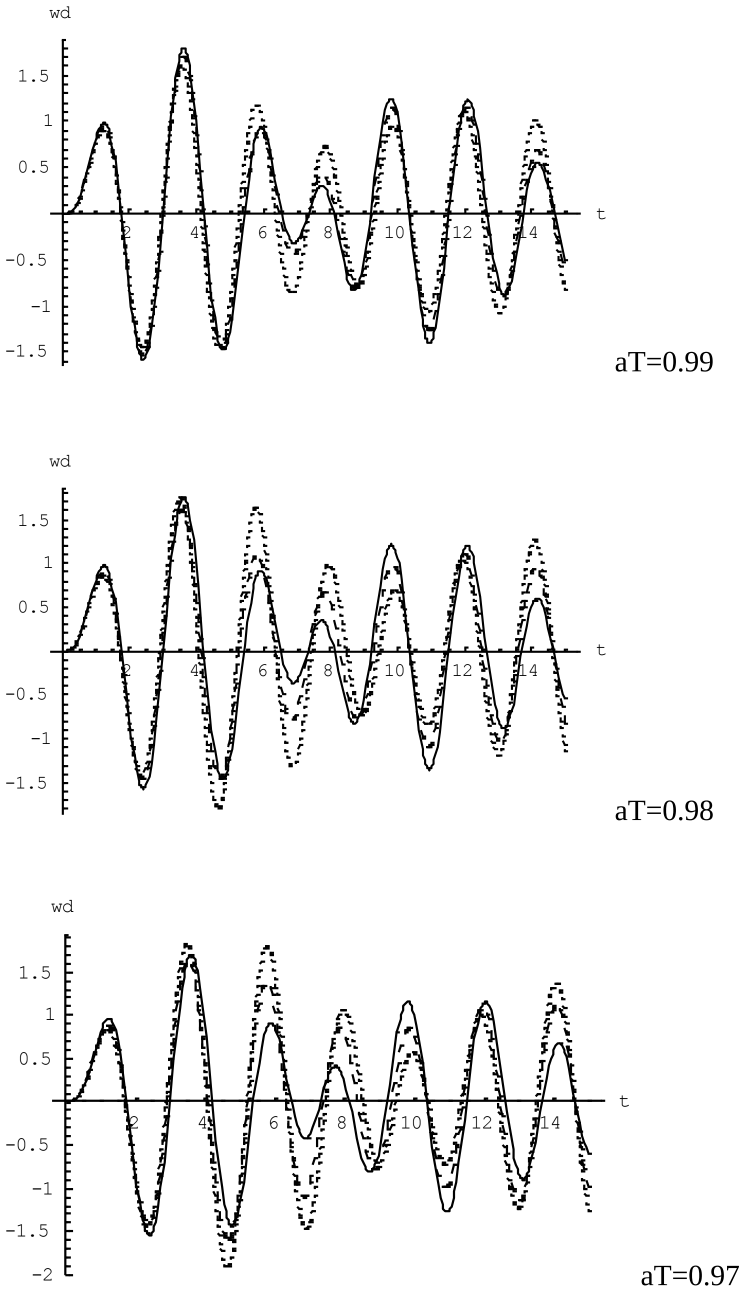

Figure 12: Cables L=350m, with dampers (___ cd=0.01, _ _ cd=0.1, - - - cd=0.5 dN sec/mm)

9. CONCLUSIONS

1. A mathematical model for the study of cables provided with dampers is proposed herein, based on the use of the real shape functions of the cable and taking into account its flexural rigidity.
2. The influence of the flexural rigidity of the cables on its dynamic behavior has proved practically negligible.
3. From the case studies examined, it is shown that the effective place to apply a damper is, usually, as far as possible from the anchorage of the cable. Furthermore, strong dampers are more effective than the soft ones.
   For some cases though, one has to study a combination of damper coefficient and its position, in order to determine the most efficient combination.
4. Even for the case of external excitations with frequencies near to one of the cable eigenfrequencies, the damping system decreases the oscillations' amplitude.

REFERENCES

[1] Fleming J.F., "Non-linear static analysis of cable-stayed bridge structures", (1979), Comp. Struct., 10, 986-1000

[2] Kollbruner C.F., Hajdin N. and Stipanic B., "Contribution to the analysis of cable-stayed Bridges", (1980), Inst. For Engineering Research Editions, Schulthess Verlag Zürich, N.48

[3] Bruno D. and Grimaldi A., "Non-linear behavior of long-span cable-stayed bridges", (1985), Meccanica, J. of the Italian Assoc. for Theoretical and Applied Mechanics, (A/META), 20(4), 303-313.

[4] Gimsing N., "Cable Supported Bridges – Concept and design", (1997), 2nd Edition, John Wiley & Sons, Chichester.

[5] Khalil M.S., "Non-linear analysis of cable-stayed bridges at ultimate load level", (1999), Canadian Jour. of Civil Engineering, 23(5), 1111-1117.

[6] Virgoreux M., "Recent evolution on cable-stayed bridges", (1999), J. of Engineering Structures, 21, 737-755.

[7] Michaltsos G.T., Ermopoulos J.C., Konstantakopoulos T.G., "Preliminary design of cable-stayed bridges for vertical static loads", (2003), J. of Structural Engineering and Mechanics, Vol. 16(1), 1-15.

[8] Freire A.M.S., Negräo J.H.O., Lopez A.V., "Geometrical non-linearities on the static analysis of highly flexible steel cable-stayed bridges", (2006), Computers and Structures, 84(31-32), 2128-2140.

[9] Fleming J.F., Egeseli E.A., "Dynamic behavior of a cable-stayed bridge", (1980), Int. Journal of Earthquake Engin. Structure Dynamics, 8(1), 1-16.

[10] Nazmy A.S. and Abdel-Ghaffar A.M., "Non-linear earthquake response analysis of long-span cable-stayed bridges", (1990), Earthquake Engineering and Structural Dynamics, 19, 45-62.

[11] Abdel-Ghaffar A.M., Khalifa M.A., "Importance of cable vibration in dynamics of cable-stayed bridges", (1991), Journal of Engineering Mechanics, 117(11), 2571-2589.

[12] Chatterjec P.K., Datta T.K., Suruna C.S., "Vibration of cable-stayed bridges under moving vehicles", (1994), Journal of Structures Ing. International, 2, 116-121.

[13] Bruno D., Colotti V., "Vibration analysis of cable-stayed bridges", (1994), Journal of Structures Ing. International, 1, 23-28.

[14] Achkire Y., Preumont A., “Active tendon control of cable-stayed bridges”, (1996), J. of Earthquake Engineering & Structural Dynamics, Vol. 25, Iss. 6, 585-597.
[15] Michaltsos G.T., “A simplified model for the dynamic analysis of cable-stayed bridges”, (2001), Facta Universitatis, V. 3, N. 11, 185-204.
[16] Konstantakopoulos T.G., Michaltsos G.T., Sophianopoulos D.S., “A simplified model for the study of the lateral-torsional vibration of cable-stayed bridges”, (2002), Eurodyn 2002, Munich.
[17] Wang P.H., liu M.Y., Huang Y.T., Lin L.C., “Influence of lateral motion of cable-stayed bridges”, (2010), Structural Engineering and Mechanics, 34(6), 719-738.
[18] Ermopoulos J., Vlahinos A., and Wang Yang-Cheng., “Stability analysis of cable-stayed bridges”, (1992), Comp. Structures, 44(5), 1083-1089.
[19] Bosdogianni A. and Olivari D., “Wind-reduced and Rain-induced oscillations of cable-stayed bridges”, (1997), Journal of wind Eng. And Industrial Aerodynamics, 64(2-3), 171-185.
[20] Michaltsos G.T., “Stability of a cable-stayed bridge’s pylon, under time-depended loading”, (2005), Collection of papers in memory of Academician P.S. Theocharis. Inst. of Mechanics Problems and Academy of Sciences, Russia, Inst. of Mechanics of Nat. Acad. of Sciences, Armenia.
[21] Michaltsos G.T., Raftoyiannis I.G., Konstantakopoulos T.G., “Dynamic Stability of cable-stayed bridge pylons”, (2008), Int. Journal of Structural Stability and Dynamics, 8(4), 627-643.
[22] Hikami, Y., Shiraishi, N., “Rain-wind-induced vibrations of cables in cable stayed bridges”, Journal of Wind Engineering and Industrial Aerodynamics, Vol. 29, Nos. 1-3, pp. 409-418, 1988.
[23] Macdonald, JHG, Dagless, EL, Thomas, BT, Taylor, CA, “Dynamic measurements of the Second Severn Crossing”, Proceedings of the Institution of Civil Engineers – Transport, Vol. 123, No. 4, pp. 241-248, 1997.
[24] Wilde, K, Witkowski, W, “Simple model of rain-wind-induced vibrations of stayed cables”, Journal of Wind Engineering and Industrial Aerodynamics, Vol. 91, No. 7, pp. 873-891, 2003.
[25] Ibrahim, RA, “Nonlinear vibrations of suspended cables – Part III: Random excitation and interaction with fluid flow”, Applied Mechanics Reviews, Vol. 57, No. 6, pp. 515-549, 2004.

Received: Sep 12, 2014 Accepted: Oct 17, 2014